Synthesis and Transport Properties of Metal Oxide Decorated Graphene Dispersed Nanofluids

ARTICLE *in* THE JOURNAL OF PHYSICAL CHEMISTRY C · APRIL 2011

Impact Factor: 4.77 · DOI: 10.1021/jp200273g

2 AUTHORS:

Tessy Baby
Indian Institute of Technology Madras
31 PUBLICATIONS **833** CITATIONS
SEE PROFILE

Ramaprabhu Sundara
Indian Institute of Technology Madras
57 PUBLICATIONS **1,121** CITATIONS
SEE PROFILE

THE JOURNAL OF PHYSICAL CHEMISTRY C

ARTICLE

pubs.acs.org/JPCC

Synthesis and Transport Properties of Metal Oxide Decorated Graphene Dispersed Nanofluids

Tessy Theres Baby and Ramaprabhu Sundara*

Alternative Energy and Nanotechnology Laboratory (AENL), Nano Functional Materials Technology Centre (NFMTC), Department of Physics, Indian Institute of Technology Madras, Chennai, India-600036

ABSTRACT: In the present work, a novel chemical reduction followed by calcination at considerably low temperature is used to synthesize copper oxide decorated graphene (CuO/HEG). Graphene has been synthesized via hydrogen induced exfoliation/reduction of graphite oxide. As-synthesized graphene is functionalized in acid medium to decorate copper oxide nanoparticles as well as to disperse it in polar medium. CuO/HEG is dispersed in deionized (DI) water and ethylene glycol without any surfactant, and the thermal transport properties of those nanofluids are studied. Thermal conductivity of CuO/HEG dispersed in DI water based nanofluid shows an enhancement of ~28% at 25 °C for a volume fraction of 0.05%. In addition to thermal conductivity, the electrical conductivity of the nanofluids is also measured for different volume fractions at different temperatures. Heat transfer coefficient is measured in an indigenously fabricated setup for different volume fractions for different flow rates.

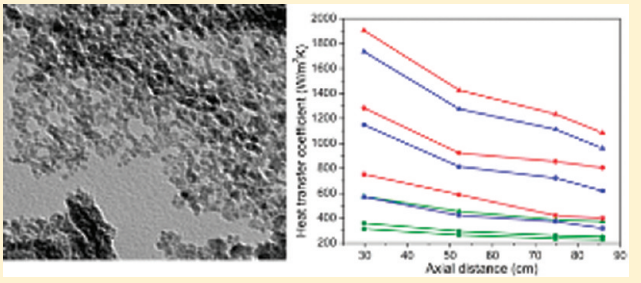

I. INTRODUCTION

It is well-known that by tuning the size of the particle one can change the property of the material and use it for different applications. In that case, nanomaterials are having tremendous scope and applications. One of the emerging fields of application of nanotechnology is the coolant industry. The conventional heat transfer fluids are water, ethylene glycol (EG), transformer oil, etc. However, the thermal conductivity of these fluids is considerably low for a good and efficient coolant. Due to the increasing global competition, there are industries that are in need of good and efficient heat transfer fluids. Since the solid materials have high thermal conductivity compared to liquids, different studies were carried out to make micro- and macromaterial dispersed fluids. Due to the problems related to clogging, sedimentation, thermal conductivity, etc., the attempt was not completely successful. Later in 1993, Choi and co-workers started thinking of a new type of fluids using nanomaterials.[1] In the same period, a Japanese group also made metal oxide dispersed nanofluids.[2] As the name indicates, these are the fluids made by dispersing nanometer sized particles in the conventional heat transfer fluids. Since the particle size is very small, the problems faced in micro- and macrofluids were not observed in nanofluids.

Compared with microparticles, nanoparticles stay suspended much longer and possess a much higher surface area. The surface/volume ratio of nanoparticles is 1000 times larger than that of microparticles. The high surface area of nanoparticles enhances the heat conduction of nanofluids, since more solid surface will take part in the heat transfer. Cu nanoparticles coated with thioglycolic acid gave a 40% increase in the thermal conductivity of EG at a particle loading of only 0.3 vol %.[3] Choi and Eastman showed a huge enhancement in thermal conductivity using copper and carbon nanotubes.[3,4] Before the introduction of nanofluids, there were different theoretical models for the enhancement of thermal conductivity and heat transfer study of solid particle dispersed fluids. However, all of them were meant for macro- and microparticles. Due to sedimentation and low thermal conductivity enhancement, theory did not match with experimental findings.[5]

In the past few years, people tried all kinds of nanomaterials to make nanofluids; some were successful, and some were not. The thermal conductivity of most of the metals is 1 or 2 orders higher than that of water. Therefore, the thermal conductivity of fluids that contain suspended solid metallic particles could be expected to be significantly higher than that of conventional heat transfer fluids. The commonly used metal oxide nanomaterials for nanofluids are TiO_2, CuO, Al_2O_3,[6−8] etc., and carbon related materials especially carbon nanotubes (CNT). Karthikeyan et al.[7] have reported an enhancement of ~31% for a 1% volume fraction of CuO nanoparticles in deionized (DI) water based nanofluid. With 3% volume fraction of TiO_2 nanoparticles, the reported value of enhancement for DI water based nanofluid was ~7.4% at 13 °C.[6] Wen et al.[9] have studied the temperature-dependent conductivity of CNT−water nanofluids.

Experimentalists have shown that nanofluids have not only better heat conductivity but also greater convective heat transfer capability than that of base fluids. The two most important parameters of a good heat transfer fluid are the stability of the

Received: January 11, 2011
Revised: March 10, 2011
Published: April 13, 2011

fluid and its high thermal conductivity. The heat transfer coefficient depends on other parameters like density, geometry of the flow, temperature, etc. Therefore, it is equally important like thermal conductivity to measure the heat transfer coefficient of nanofluids. There are experimental studies on the heat transfer properties of Al_2O_3, TiO_2, and CuO nanoparticles.[10−12] Ding et al.[13] showed the enhancement in heat transfer property of CNT dispersed based nanofluid. Xie[14] proposed a method to produce stable and homogeneous suspensions of CNT in DI water, EG, and decene (DE).

The one atom thick graphene is the most widely used nanomaterial because of its excellent properties. Graphene has high electrical conductivity, high mobility of charge carriers, high thermal conductivity, high mechanical strength, extremely large surface area, etc.[15] Moreover, graphene is easy to synthesize and the cost of synthesis is less compared to other nanomaterials. Thus, graphene and graphene based nanocomposites are extensively used in different applications such as fuel cells, lithium ion batteries, biosensors, gas sensors, etc.[16−19] The property of graphene is slightly varying the way in which it makes and the number of graphene sheets present. There are different methods to make single layer and few layer graphene, namely, micromechanical cleavage,[15] chemical vapor deposition,[20] exfoliation of graphite oxide,[21,22] etc. The experimentally calculated thermal conductivity of single layer graphene was $\sim(4.84 \pm 0.44) \times 10^3$ to $(5.30 \pm 0.48) \times 10^3$ W/mK.[23] This value is higher than the thermal conductivity of CNT.

In our previous paper, we reported the enhancement in thermal conductivity of thermally exfoliated graphene dispersed nanofluids. The water based nanofluid shows an enhancement of ~14% for a volume fraction of 0.056%.[24] Recently, we have synthesized graphene via a novel technique called hydrogen induced exfoliated graphene (HEG).[22] The thermal conductivity and heat transfer of these nanomaterial dispersed nanofluids are reported in our previous work.[25] The results claim that such nanofluids can be used for coolant applications.

There are several reports on the enhancement in thermal conductivity of different metal/metal oxide decorated CNT composite dispersed nanofluids.[26,27] Being the highest thermal conductive material among the whole carbon family, graphene and its nanocomposites also can be used for such applications. This motivated us to make graphene nanocomposite dispersed nanofluids. In the present work, CuO decorated graphene (CuO/HEG) is synthesized by hydrogen induced exfoliation of graphite oxide (GO) followed by chemical reduction. The as synthesized HEG was functionalized with acid treatment and further used for coating CuO and making nanofluid. The thermal conductivity and heat transfer coefficient of those nanofluids were measured systematically. To the best of our knowledge, no work has been reported on the heat transfer and thermal conductivity of CuO/HEG dispersed nanofluids except some reports only on the synthesis of CuO/graphene.[28,29]

II. EXPERIMENTAL SECTION

A. Material Synthesis. Graphite (99.99%, 45 μm) was purchased from Bay Carbon, Inc. USA. All other reagents like sulphuric acid, nitric acid, $KMnO_4$, sodium nitrate, silver nitrate, sodium borohydride ($NaBH_4$), copper chloride, sodium hydroxide (NaOH), ethylene glycol and H_2O_2 were analytical grade. DI water was used throughout the experiment.

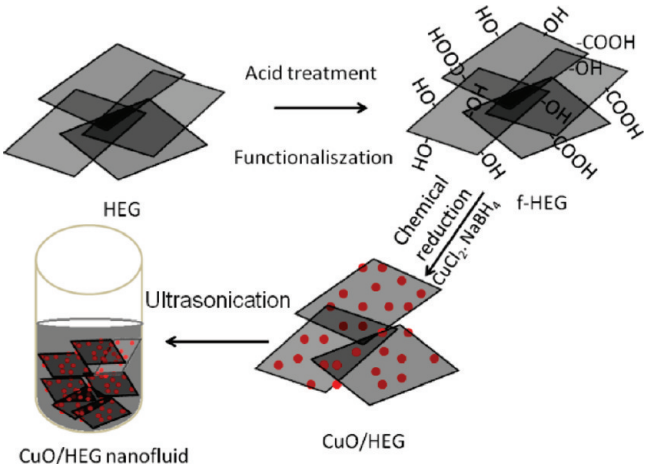

Figure 1. Schematic of the synthesis of CuO/HEG and thereafter making of nanofluid using this nanocomposite.

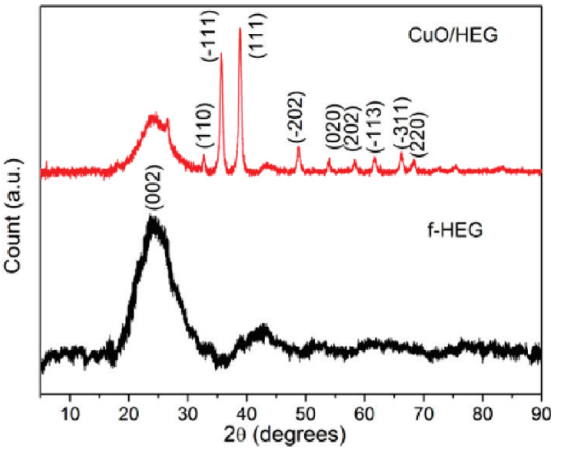

Figure 2. X-ray diffraction analysis of f-HEG and CuO/HEG.

The synthesis procedure of HEG was explained in our previous report.[22] Since the as grown graphene was hydrophobic in nature, it was impossible to disperse it in any polar solvents. In order to make it hydrophilic, acid treatment was carried out. This process is called functionalization of graphene. The main aim of functionalization was to introduce carboxyl and hydroxyl functional groups on the surface of graphene. Functionalization was done by treating as grown HEG in a 3:1 ratio of H_2SO_4 and HNO_3 solution for 3 h under ultrasonication. After 3 h, the mixture was washed with DI water and then filtered and dried. The functionalized graphene (f-HEG) was used to decorate the CuO nanoparticles. For convenience, we did a 20% coating of CuO nanoparticles on f-HEG by chemical reduction and the synthesis procedure was as follows. The f-HEG was dispersed in DI water by ultrasonication followed by stirring. A specific amount of $CuCl_2$ solution was added to the above solution under stirring. Stirring was continued for 12 h, and after that, a reducing solution which was a mixture of $NaBH_4$ and NaOH was added to the previous solution. After completion of the reducing solution, the colloidal solution was washed well with DI water, filtered, and dried. This sample was used to make nanofluid. A calculated amount of CuO/HEG was dispersed in the base fluids (DI water or ethylene glycol) by ultrasonication. The ultrasonication

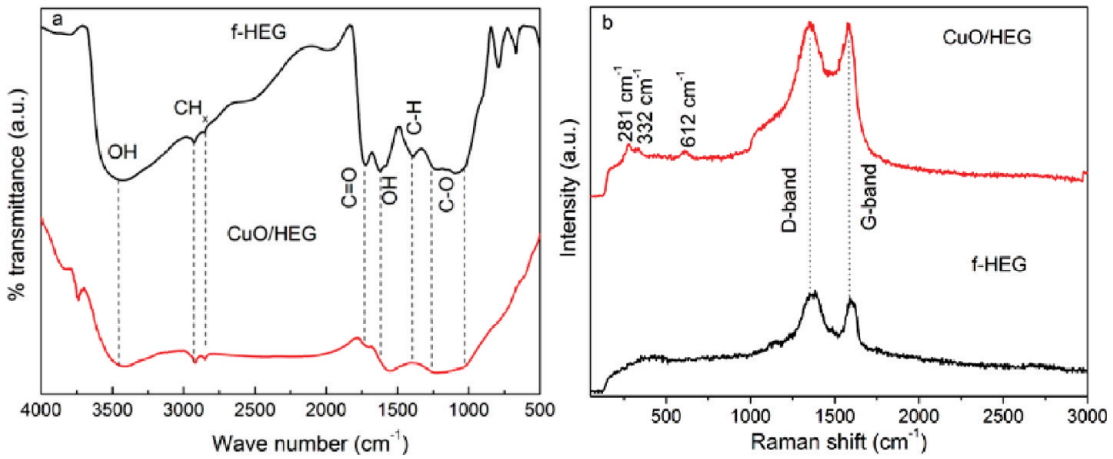

Figure 3. (a) Fourier transform infrared spectra and (b) Raman spectra of f-HEG and CuO/HEG.

time was optimized to 45 min to 1 h. A schematic of the sample synthesis and thereafter making of nanofluid is shown in Figure 1.

B. Experimental Techniques. Powder X-ray diffraction studies were carried out using a PANalytical X'PERT Pro X-ray diffractometer with nickel-filtered Cu Kα radiation as the X-ray source. The pattern was recorded in a 2θ range of 5−90° with a step size of 0.016°. Identification and characterization of functional groups on the surface of f-HEG and Ag/HEG were carried out using a PerkinElmer FT-IR spectrometer in the range 500−4000 cm^{-1}. The Raman spectra were obtained with a WITEC alpha 300 Confocal Raman system equipped with a Nd:YAG laser (532 nm) as the excitation source. The intensity was kept at a minimum to avoid laser induced heating. The morphology of the samples was characterized by field emission scanning electron microscopy (FESEM, FEI QUANTA). Transmission electron microscopy (TEM) was carried out using a JEOL JEM-2010F microscope. For TEM measurements, the graphene powder was dispersed in absolute ethanol using mild ultrasonication and casted onto carbon coated Cu grids (SPI supplies, 200 mesh). The thermal conductivity of the suspension was measured using a KD2 pro thermometer (Decagon, Canada). The probe sensors used for these measurements are of length 6 cm and of diameter 1.3 mm. In order to study the temperature effect on the thermal conductivity of nanofluid, a thermostat bath was used. The electrical conductivity of the nanofluids was measured using a CM 183 ELICO meter.

The convective heat transfer mechanism was studied using an indigenously fabricated setup. A schematic of the setup is given in ref 25. It consists of a flow loop, a heat unit, a cooling part (heat exchanger), and a measuring and control unit. The flow loop included a pump with flow controlling valve system, a reservoir, a collection tank, and a test section. A straight stainless steel tube with 108 cm length and 23 mm inner diameter was used as the test section. The whole test section was heated by a copper coil linked to an adjustable DC power supply. There was a thick thermal isolating layer surrounding the heater to obtain a constant heat flux condition along the test section. Four T-type thermocouples were mounted on the test section at axial positions in mm of 298 (T1), 521 (T2), 748 (T3), and 858 (T4) from the inlet of the test section to measure the wall temperature distribution, and two further T-type thermocouples were inserted into the flow at the inlet and exit of the test section to measure the bulk temperatures of the nanofluids. The role of the heat exchanger was to cool down the nanofluid coming out from the outlet of the test section.

III. RESULTS AND DISCUSSION

A. Material Characterization. The formation as well as crystallinity of the samples is first studied using X-ray diffraction (XRD). Figure 2 shows the XRD of f-HEG and CuO/HEG. In f-HEG, the (002) plane of graphite is shifted slightly to the left and becomes broad too. Now the peak position is ∼24.5° instead of 26.5°. In the case of CuO/HEG, in addition to the graphite peak, there are peaks corresponding to CuO also. The peak at ∼38.8, 35.6, 48.8, 53.8, 58.3, 61.7, 66.3, and 68.3° corresponds to the (111), (−111), (−202), (020), (202), (−113), (−311), and (220) planes of CuO nanoparticles.[28] The crystalline size of the CuO nanoparticle is calculated using Scherrer's formula for the peak 38.8°, and it is ∼8.5 nm. The XRD pattern demonstrates that CuO/HEG is successfully synthesized by the chemical reduction technique.

Figure 3a shows the Fourier transform infrared (FTIR) spectroscopy of f-HEG and CuO/HEG. This gives an idea of the functional groups present on the surface of f-HEG and CuO/HEG. As seen in the figure, the curve f-HEG is rich in hydroxyl and carboxyl groups. The peak around 3441 and 1620 cm^{-1} corresponds to the O—H group and a doublet peak between 2850 and 2930 cm^{-1} corresponds to asymmetric stretching and symmetric vibrations of the CH_2 group. The vibration peak at ∼1727 cm^{-1} corresponds to C═O of the carboxyl group.[22] The peak around 1392 and 1259 cm^{-1} corresponds to C—H and C—O groups. In the case of CuO/HEG, the functional group intensities were reduced compared to f-HEG. This confirms the formation of CuO/HEG. The functional groups help decorate metal/metal oxide nanoparticles on the surface of graphene as well as help for proper dispersion of graphene in the polar base fluid. Figure 3b shows the Raman spectra of f-HEG and CuO/HEG. The two prominent peaks at ∼1591 and 1367 cm^{-1} represent the G-band and D-band, respectively. The G-band is the characteristic sp^2 vibration of most of the carbon based materials. In another way, this peak is due to the in plane vibration of carbon atoms present in the sample. The D-band can be due to the presence of disorder, impurities, or defects in the sample. Sometimes the metal/metal oxide coating on carbon based materials gives a D-band. In the present case, the D-band

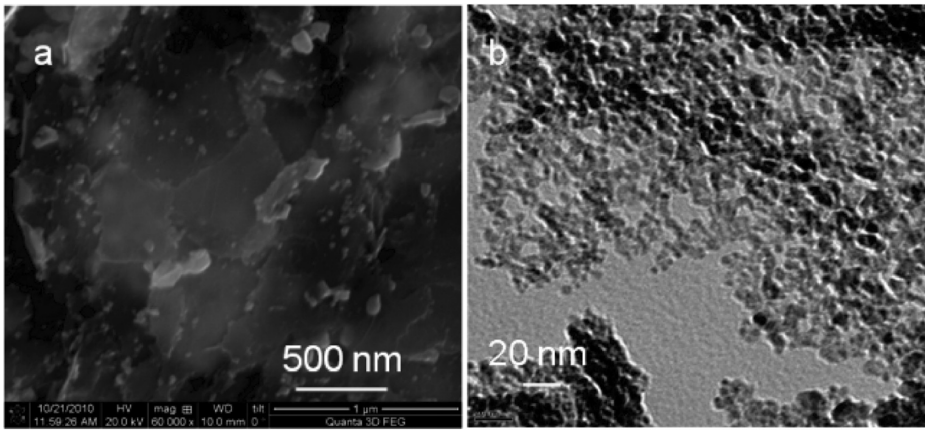

Figure 4. (a) FESEM and (b) TEM images of CuO/HEG.

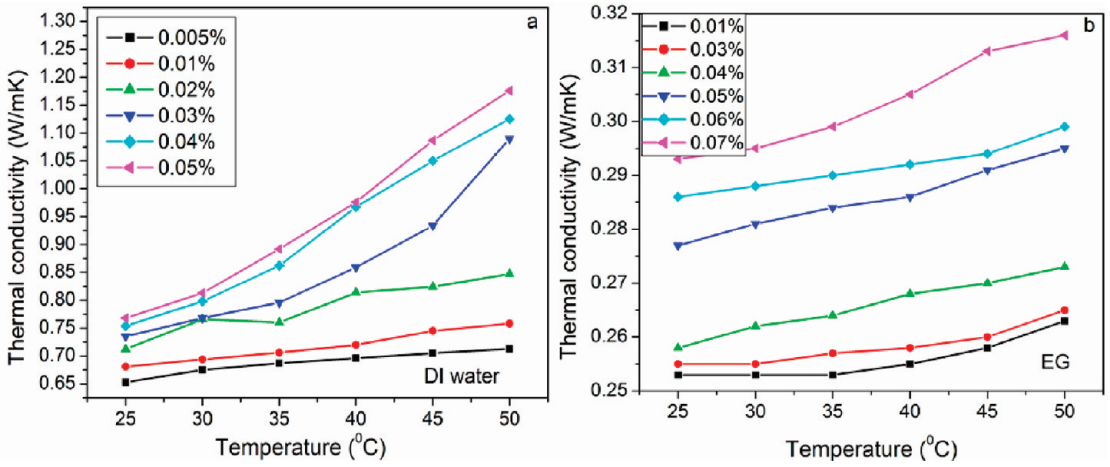

Figure 5. Thermal conductivity of (a) DI water and (b) ethylene glycol based CuO/HEG dispersed nanofluids with respect to temperature for different volume fractions.

can be due to the sp^3 disorder formed due to functionalization and also due to the wrinkled morphology of graphene. The Raman spectrum of CuO/HEG shows three extra peaks below 1000 cm^{-1} in addition to the G-band and D-band. The extra peak at ~281, 332, and 612 cm^{-1} corresponds to one A_g and two B_g modes of vibrations of CuO.[29] There is a small shift in the D-band (1347 cm^{-1}) and G-band (1576 cm^{-1}) for CuO/HEG compared to f-HEG. The presence of additional peaks and shift in G-band and D-band once again confirms the formation of CuO/HEG.

Parts a and b of Figure 4 show the FESEM and TEM images of CuO/HEG, respectively. The surface morphology of CuO/HEG and f-HEG is more or less clear from the FESEM image. The particle size calculated from the TEM image is nearly matching with what we calculated in XRD using the Scherrer equation. The TEM image shows a uniform coating of CuO nanoparticles on HEG. The TEM image was taken after dispersing a small amount of CuO/HEG in ethanol by ultrasonication. The image shows that even after the ultrasonication the nanoparticles remain on the graphene sheets.

B. Thermal and Electrical Conductivity. As we mentioned earlier, nanofluids are made by dispersing specific quantities of CuO/HEG in DI water and EG. The thermal conductivity of these fluids is measured for different volume fractions at different temperatures. Figure 5a shows the thermal conductivity of DI water based nanofluids at different temperatures for different concentrations. The selection of low volume fractions of CuO/HEG for the study is to avoid enhancement in the viscosity. As seen in the graph, the thermal conductivity of the nanofluid is increasing with temperature as well as with volume fraction. The increase in thermal conductivity is nonlinear both for temperature and for volume fraction. The linearity/nonlinearity of thermal conductivity with respect to volume fraction depends on the nature of the nanoparticle as well as the base fluid. The percentage in thermal conductivity (k_e) is calculated using the formula

$$\% = [(k - k_0) \times 100]/k_0 \quad (1)$$

where k_0 is the thermal conductivity of the base fluid and k is that of the nanofluid.

For 0.05% volume fraction of CuO/HEG, the enhancement in thermal conductivity is ~28% at 25 °C. Almost 90% enhancement is observed for the same volume fraction at 50 °C. This behavior of nonlinearity and enhancement is matching with other literature reports.[8] This enhancement in thermal conductivity can be due to the high thermal conductivity of graphene as well as copper oxide nanoparticles. When volume fraction

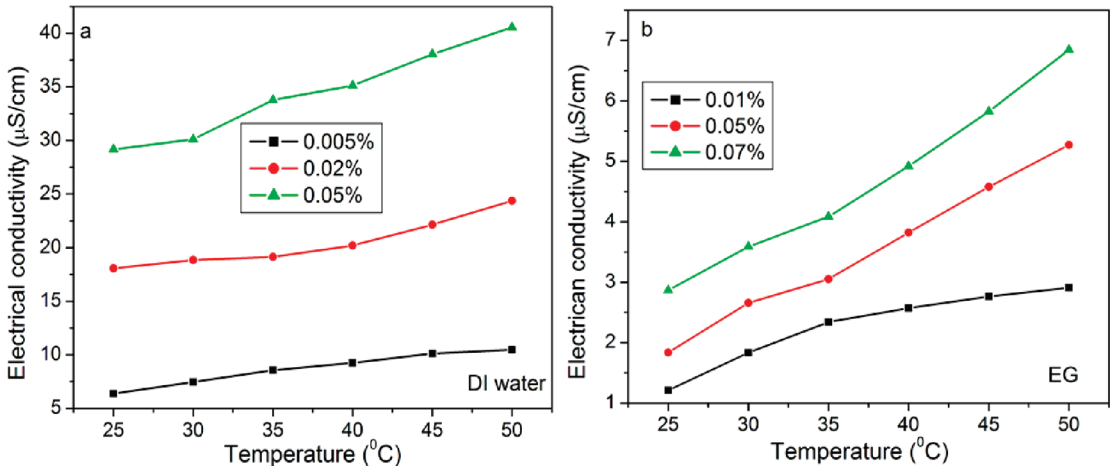

Figure 6. Electrical conductivity of (a) DI water and (b) ethylene glycol based CuO/HEG dispersed nanofluids with respect to temperature for different volume fractions.

increases, the particle−particle distance (in other words, mean free path) decreases. This is due to the percolation effect. More particles are in contact with each other, which increases the frequency of lattice vibration.

The thermal conductivity of CuO/HEG dispersed in EG based nanofluid with respect to temperature for different volume fractions is shown in Figure 5b. A similar trend in thermal conductivity is observed for EG based nanofluids also. However, unlike DI water based nanofluids, the enhancement in thermal conductivity is less for EG based nanofluids with respect to temperature and volume fraction. The enhancement in thermal conductivity is ∼17% at 25 °C for a volume fraction of 0.07%, and that at 50 °C is ∼23%. The enhancement in thermal conductivity is not very high, as we have expected. This can be due to the sp^3 defects formed in the graphene sheets.

Similarly, the electrical conductivities of DI water and EG based nanofluids are also measured at different temperatures for different volume fractions. The results of DI water and EG based nanofluids are shown in parts a and b of Figure 6, respectively. We have observed an enhancement in electrical conductivity with respect to temperature and volume fraction both in the case of DI water based and EG based nanofluids. Since CuO is not a good electrical conductor, the electrical conductivity is not as high as that of f-HEG.[25]

C. Convective Heat Transfer. The heat transfer coefficient, h, is a macroscopic parameter describing heat transfer when a fluid is flowing across a solid surface of different temperature. It is not a material property. The convective heat transfer coefficient is defined as

$$h = \frac{q}{(T_s(x) - T_f(x))} \tag{2}$$

where x represents the axial distance from the entrance of the test section, q is the heat flux, T_s is the measured wall temperature, and T_f is the fluid temperature decided by the following energy balance:

$$T_f(x) = T_{in} + \frac{E(x)}{Mc_p} \tag{3}$$

where c_p is the heat capacity, M is the mass flow rate, and $E(x)$ is the energy at position x. Equation 2 is based on an assumption of zero heat loss through the insulation layer.

$$E(x) = \frac{(\text{total energy} \times x)}{\text{length of the tube}} \tag{4}$$

And mass flow rate can be calculated using the relation

$$M = uA\rho \tag{5}$$

where u is the velocity of flow, A is the area of cross section, and ρ is the density of fluid. The Reynolds number is defined as $Re = (\rho uD)/(\mu)$ and the Prandtl number is defined as $Pr = (\nu)/(\alpha)$, where μ is the fluid dynamic viscosity, ν is the fluid kinematic viscosity, and α is the fluid thermal diffusivity.

D. Validity of the Experimental Setup with DI Water. To check the reliability and accuracy of the fabricated experimental setup, systematic measurements were carried out using distilled water as the working fluid for both laminar flow and turbulent flow. The experimental results obtained by laminar flow and high turbulent flow are correlated with the well-known Shah correlation[30] and Dittus−Boelter equation,[31] respectively, under the constant heat flux boundary condition. The famous Shah correlation is

$$Nu = \begin{cases} 1.953(\mathrm{RePr}\frac{D}{x})^{\frac{1}{3}} & (\mathrm{RePr}\frac{D}{x}) \geq 33.3 \\ 4.364 + 0.0722\mathrm{RePr}\frac{D}{x} & (\mathrm{RePr}\frac{D}{x}) < 33.3 \end{cases} \tag{6}$$

where Nu is the Nusselts number. The experimental values are reasonably in good agreement with the Shah equation, as shown in Figure 7a. The same was observed for other laminar flow rates also. Similarly for high turbulent flow, the Dittus−Boelter equation is given below:

$$Nu = 0.023Re^{0.8}Pr^{0.4} \tag{7}$$

As shown in Figure 7b, the good coincidence between the experimental results and the calculated values for water reveals that the precision of the experimental system is considerably good. The uncertainty of the experimental system is less than 5%.

E. Experimental Study of Heat Transfer Using CuO/HEG Nanofluid. Heat transfer study of CuO/HEG nanomaterial dispersed nanofluids is carried out for DI water and EG based fluids. The experiment is conducted for two considerably low

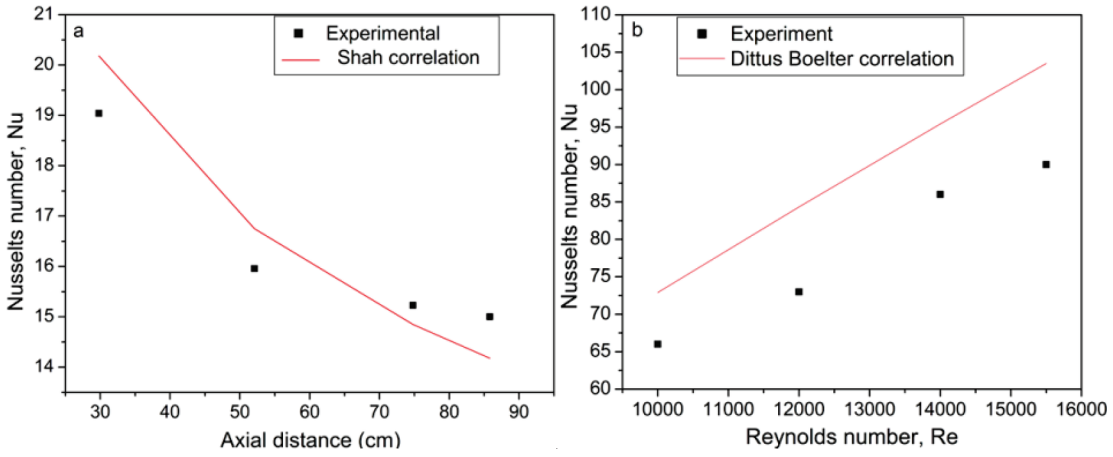

Figure 7. Validity of the experimental heat transfer setup for (a) low (Shah correlation) and (b) high (Dittus−Boelter correlation) flow rates using water.

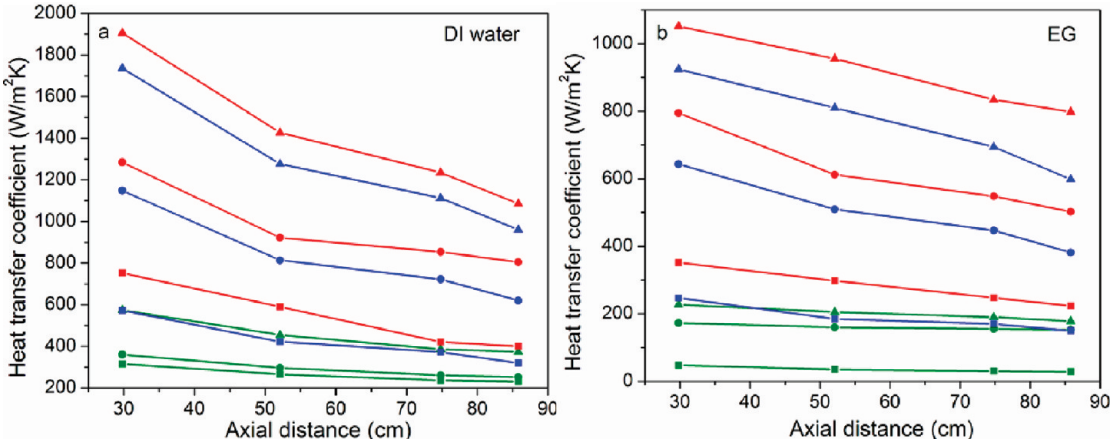

Figure 8. Heat transfer study of (a) DI water and (b) ethylene glycol based CuO/HEG dispersed nanofluids. The green, blue, and red solid lines correspond to the heat transfer of base fluid alone, 0.005% volume fraction of CuO/HEG in base fluid, and 0.01% of CuO/HEG in base fluid, respectively. The symbols ■, ●, and ▲ represent *Re* = 4500, 8700, and 15500, respectively, for DI water and *Re* = 250, 550, and 1000, respectively, for ethylene glycol based nanofluids.

volume fractions (0.005 and 0.01%) and different Reynolds numbers. Figure 8a shows the heat transfer study of DI water based nanofluids for different volume fractions and different Reynolds numbers. In the graph, the green line represents the heat transfer of DI water alone, blue for 0.005% volume fraction of CuO/HEG in DI water, and red for 0.01% volume fraction of CuO/HEG in DI water. The solid square symbol represents *Re* = 4500, the solid circle represents *Re* = 8700, and the solid triangle represents *Re* = 15500. In other words, the flow is considered to be turbulent. It is clear from the graph that heat transfer is increasing with respect to volume fraction as well as Reynolds number. For a particular volume fraction and Reynolds number, the heat transfer coefficient is decreasing when going from the entrance of the heat pipe to the exit of the heat pipe. The percentage enhancement in heat transfer coefficient is calculated using the equation

$$\% = \frac{[h(x) - h_n(x)]}{h(x)} \times 100 \qquad (8)$$

where $h(x)$ and $h_n(x)$ are the heat transfer coefficients for the base fluid and nanofluid at distance x. The percentage enhancement in heat transfer for a volume fraction of 0.005% in a Reynolds number of 4500 is ∼81%, and that for *Re* = 15500 is ∼202% at the entrance of the heat pipe. At the exit, the heat transfer decreases to ∼39 and ∼156%, respectively, for *Re* = 4500 and *Re* = 15500 for the same volume fraction. When the volume fraction of CuO/HEG increased the 0.01% the enhancement is more. For *Re* = 4500 and 15500, the enhancement in heat transfer is ∼138 and ∼232%, respectively, at the entrance of the heat pipe. At the exit of the pipe, the enhancement decreases to ∼74 and ∼190%, respectively, for *Re* = 4500 and 15500.

Similarly, heat transfer studies are carried out for EG based nanofluid also and are shown in Figure 8b. For EG based nanofluids, the Reynolds numbers selected are *Re* = 250, 550, and 1000. The flow is considered to be laminar flow. The two volume fractions used are 0.005 and 0.01%. In the graph, the green solid line, blue solid line, and red solid line represent EG alone, 0.005% volume fraction of CuO/HEG in EG, and 0.01% volume fraction of CuO/HEG in EG, respectively. Similar to water based nanofluids, the symbols square, circle, and triangle represent *Re* = 250, 550, and 1000, respectively. The same eq 8 is used to calculate percentage enhancement in heat transfer coefficient. The heat

dx.doi.org/10.1021/jp200273g |*J. Phys. Chem. C* 2011, 115, 8527–8533

transfer coefficient is increasing with respect to volume fraction and Reynolds number in this case also. The enhancement in heat transfer is more for EG based nanofluids.

Unlike thermal conductivity, the enhancement in convective heat transfer is huge for both DI water and EG based nanofluids. The enormous enhancement in heat transfer suggests that there are other factors like particle size, type, dispersion, and chaotic movement of nanoparticles, Brownian motion, particle migration, and nanofluid viscosity involved in the convective heat transfer mechanism.[32] As we mentioned earlier, the percolation of nanomaterials may be the reason for enhancement in heat transfer for high volume fractions. The reason for the decrease in heat transfer coefficient from the entrance to the exit of the tube is due to the variation of the thermal boundary layer. In a simple way, heat transfer can be written as k/δ, with δ being the thickness of the thermal boundary layer. At the entrance $(x = 0)$, the theoretical boundary layer thickness is zero; hence, the heat transfer coefficient approaches infinity. The boundary layer increases with axial distance until fully developed after which the boundary layer thickness and hence the convective heat transfer coefficient are constant.[13] To interpret the experimental results and deviation from the theoretical equations, it should be noted that the enhancement of heat transfer greatly depends on particle type, particle size, base fluid, flow regime, and especially boundary condition. The presence of nanoparticles in fluid changes the flow structure so that besides thermal conductivity increment, chaotic movements, dispersions, and fluctuations of nanoparticles especially near the tube wall lead to an increase in the energy exchange rates and augment the heat transfer rate between the fluid and the tube wall.

Both the thermal conductivity and heat transfer coefficient of CuO/HEG nanofluids are higher than those of f-HEG nanofluids.[25] This can be due to the effect of CuO nanoparticles in the composite which avoids the stacking of graphene layers to some extent and also helps to increase the surface area of the nanocomposite. Moreover, the electrical conductivity of CuO/HEG nanofluids is less than that of f-HEG nanofluids and hence CuO/HEG nanofluids may be used as coolant fluid in engines as well as in electrical circuits.

IV. CONCLUSION

CuO decorated on hydrogen induced exfoliated graphene is synthesized successfully. CuO/HEG dispersed nanofluids are synthesized both in DI water and ethylene glycol base fluids without any surfactant. Experimental study on the thermal conductivity and heat transfer suggests that these nanofluids can be used for coolant applications. Moreover, the cost of graphene is less compared to any other carbon based nanomaterial. The electrical conductivity measurements on these nanofluids give even wider applications for these nanofluids. The low enhancement in electrical conductivity of nanofluid can be utilized in insulating fluid applications. More experiments are needed for a better understanding of the mechanism of the enhancement in thermal conductivity and heat transfer.

AUTHOR INFORMATION

Corresponding Author

*Phone: +91-44-22574862. Fax: +91-44-22570509. E-mail: ramp@iitm.ac.in.

ACKNOWLEDGMENT

The authors would like to thank DRDO and IIT Madras, India, for financial support for the present work. The authors would also like to thank Sophisticated Analytical Instrument Facility (SAIF) IIT Madras for FTIR analysis.

REFERENCES

(1) Choi, S. U. S. FED-231/MD-66; ASME: New York, 1995; p 99.
(2) Masuda, H.; Ebata, A.; Teramae, K.; Hishinuma, N. *Netsu Bussei* **1993**, *4*, 227.
(3) Eastman, J. A.; Choi, S. U. S.; Li, S.; Yu, W.; Thompson, L. J. *Appl. Phys. Lett.* **2001**, *78*, 718.
(4) Choi, S. U. S.; Zhang, Z. G.; Yu, W.; Lockwood, F.; Grulke, E. A. *Appl. Phys. Lett.* **2001**, *79*, 2252.
(5) Maxwell-Garnett, J. C. *Philos. Trans. R. Soc., A* **1904**, *203*, 385.
(6) Turgut, A.; Tavman, I.; Chirtoc, M.; Schuchmann, H. P.; Sauter, C.; Tavman, S. *Int. J. Thermophys.* **2009**, *30*, 1213.
(7) Karthikeyan, N. R.; Philip, J.; Baldev, R. *Mater. Chem. Phys.* **2008**, *109*, 50.
(8) Das, S. K.; Putra, N.; Thiesen, P.; Roetzel, W. *J. Heat Transfer* **2003**, *125*, 567.
(9) Wen, D. S.; Ding, Y. L. *J. Thermophys. Heat Transfer* **2004**, *18*, 481.
(10) Sundar, L. S.; Sharma, K. V.; Ramanathan, S. *Int. J. Nanotechnol.* **2007**, *1*, 21.
(11) Lee, S.; Choi, S. U. -S.; Li, S.; Eastman, J. A. *J. Heat Transfer* **1999**, *121*, 280.
(12) Nassan, T. H.; Heris, S. Z.; Noie, S. H. *Int. Commun. Heat Mass Transfer* **2010**, *37*, 7924.
(13) Ding, Y.; Alias, H.; Wen, D.; Williams, R. A. *Int. J. Heat Mass Transfer* **2006**, *49*, 240.
(14) Xie, H.; Lee, H.; Youn, W.; Choi, M. *J. Appl. Phys.* **2003**, *94*, 4967.
(15) Novoselov, K. S.; Geim, A. K.; Morozov, S. V.; Jiang, D.; Zhang, Y.; Dubonos, S. V.; Grigorieva, I. V.; Firsov, A. A. *Science* **2004**, *306*, 666.
(16) Seger, B.; Kamat, P. V. *J. Phys. Chem. C* **2009**, *113*, 7990.
(17) Su, F. −Y.; You, C.; He, Y. −B.; Lv, W.; Cui, W.; Jin, F.; Li, B.; Yang, Q. −H.; Kang, F. *J. Mater. Chem.* **2010**, *20*, 9644.
(18) Baby, T. T.; Aravind, S. S. J.; Arockiadoss, T.; Rakhi, R. B.; Ramaprabhu, S. *Sens. Actuators, B* **2010**, *145*, 71.
(19) Kaniyoor, A.; Jafri, R. I.; Arockiadoss, T.; Ramaprabhu, S. *Nanoscale* **2009**, *1*, 382.
(20) Land, T. A.; Michely, T.; Behm, R. J.; Hemminger, J. C.; Comsa, G. *Surf. Sci.* **1992**, *264*, 261.
(21) Tung, V. C.; Allen, M. J.; Yang, Y.; Kaner, R. B. *Nat. Nanotechnol.* **2009**, *4*, 25.
(22) Kaniyoor, A.; Baby, T. T.; Ramaprabhu, S. *J. Mater. Chem.* **2010**, *20*, 8467.
(23) Balandin, A. A.; Ghosh, S.; Bao, W.; Calizo, I.; Teweldebrhan, D.; Miao, F.; Lau, C. N. *Nano Lett.* **2008**, *8*, 902.
(24) Baby, T. T.; Ramaprabhu, S. *J. Appl. Phys.* **2010**, *108*, 124308.
(25) Baby, T. T.; Ramaprabhu, S. *Nanoscale Res. Lett.*, **2011** *6*, 289.
(26) Han, Z. H.; Yang, B.; Kim, S. H.; Zachariah, M. R. *Nanotechnology* **2007**, *18*, 105701.
(27) Jha, N.; Ramaprabhu, S. *J. Phys. Chem. C* **2008**, *112*, 9315.
(28) Mai, Y. J.; Wang, X. L.; Xiang, J. Y.; Qiao, Y. Q.; Zhang, D.; Gu, C. D.; Tu, J. P. *Electrochim. Acta* **2011**, *56*, 2306.
(29) Zhu, J.; Zeng, G.; Nie, F.; Xu, X.; Chen, S.; Han, Q.; Wang, X. *Nanoscale* **2010**, *2*, 988.
(30) Shah, R. K. Proc. 3rd National Heat Mass Transfer Conference. Indian Institute of Technology, Bombay, 1975, 1, HMT-11-75.
(31) Dittus, F. W.; Boelter, L. M. K. *University of California, Berkeley, Publications on Engineering* **1930**, *2*, 443.
(32) Lee, D.; Kim, J. −W.; Kim, B. G. *J. Phys. Chem. B* **2006**, *110*, 4323.